

Antireflective characteristics of triangular shaped gratings

Jianguo Wang (王建国), Jianda Shao (邵建达), Sumei Wang (王素梅),
Hongbo He (贺洪波), and Zhengxiu Fan (范正修)

Shanghai Institute of Optics and Fine Mechanics, Chinese Academy of Sciences, Shanghai 201800

Received January 17, 2005

The antireflection properties of triangular shaped gratings are studied by a combination of the effective medium theory and the anisotropic thin-film theory. The triangular shaped structures are analyzed as a function of grating period, filling factor, and groove depth, and the antireflective characteristics are also studied when visible-infrared light is incident upon them. Numerical examples are given for gratings on glass substrate with refractive index of 1.5. The results show that this kind of grating is capable of reducing reflections, and could achieve very low reflectivity over a wide field of view and a wide waveband by choosing appropriate parameters.

OCIS codes: 050.1950, 050.1960, 220.4000, 310.1210.

It is well known that conventional multi-layers are often used for antireflective coatings^[1,2]. There are, however, only a handful of optical materials available, thus limiting the performance that could ideally be achieved. On the other hand, sub-wavelength structure surfaces, which are surface-relief gratings with periods smaller than the incident wavelength, have been researched and found to have antireflective properties^[3-8]. Compared with standard optical thin-film coating technologies, the high spatial frequency grating antireflective microstructure provides the advantages of durability, damage resistivity, and the ability to substitute materials of specific characteristics that are unsuitable or unavailable in thin-film form. The areas of their applications include high-power lasers, solar cells, and photodetectors.

In the long-wavelength limit, when the incident light wavelength is large compared with the grating period, the rectangular-groove, surface-relief grating shows birefringence^[9] and produces only a zeroth diffraction order. In this limit the grating is equivalent to an anisotropic homogeneous layer, and a combination of the effective-medium theory and anisotropic thin-film theory may be applied^[7]. An effective grating model, generalized from effective medium theory, is developed to explain the Bragg behavior of resonance domain surface-relief gratings^[10]. Their model also involves the approximation of the refractive index distribution with thin sublayers of surface-relief grating. The antireflective characteristics of rectangular-grooved and V-grooved gratings have been identified previously^[7,8]. However, to our knowledge, there have been no theoretical studies on the triangular shaped sub-wavelength surface relief gratings. In this paper we use the effective medium theory and the anisotropic thin-film theory to analyze and calculate the characteristics of the triangular shaped grating. The results show that this kind of grating is capable of reducing reflections and we can get very low reflectivity by choosing appropriate parameters.

A triangular shaped grating is specified by the parameters shown in Fig. 1: groove depth d , grating period Λ , refractive index of the grating n_1 , and grating vector \mathbf{K} , which is normal to the grooves. The light wave is incident from the ambient medium of refractive index n_0

at angle θ_0 to the surface normal. Refractive angle θ_2 in the substrate is determined by Snell's law. The ambient and substrate media are supposed to be homogeneous and isotropic dielectrics. A single period of a triangular shaped grating is divided into a large number of planar layers, as depicted in Fig. 2. Figure 3 illustrates the correspondent thin-film equivalent of the grating in Fig. 1, represented by a stack of thin layers with the total thickness identical to the grating-region thickness but with different equivalent refractive indices for each layer: $n(m)_{E\parallel K}$, and $n(m)_{E\perp K}$ for TM and TE polarizations, respectively, where $m = 1, 2, \dots, N$, N is the total number of layers.

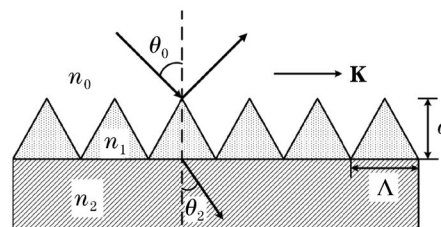


Fig. 1. Dielectric triangular shaped grating in cross section. The grating is characterized by the incident medium, grating medium, and substrate medium with refractive indices n_0 , n_1 , and n_2 , respectively, the grating medium thickness of d and grating period of Λ . The incident wave vector makes a polar angle θ_0 from the surface normal.

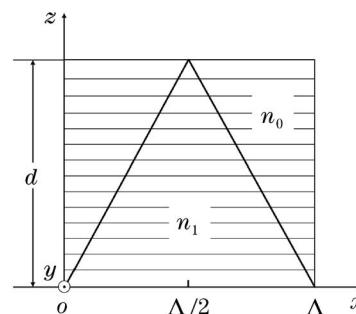


Fig. 2. Geometry of triangular shaped grating and its decomposition into a stack of thin layers.

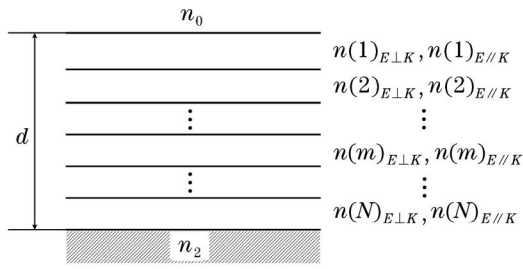


Fig. 3. Schematic diagram of equivalent homogeneous multi-layer model of the triangular shaped grating.

The thickness of each layer is d/N , and the filling factor for the m -th layer is

$$F_m = m/N. \tag{1}$$

A normally incident electromagnetic wave of wavelength λ is either TE polarized or TM polarized. At normal incidence, when λ is large compared with grating period Λ , the grating can be characterized by two equivalent refractive indices, $n_{E\parallel K}$ and $n_{E\perp K}$, depending on the orientation of the electric field \mathbf{E} of the incident wave parallel or perpendicular to the grating vector \mathbf{K} . In general, $n_{E\parallel K}$ and $n_{E\perp K}$ are determined by the solution of the transcendental equations^[11] derived under the conditions of normal incidence and non-static electromagnetic-field distribution in the grating structure. As the period-to-wavelength ratio Λ/λ becomes larger, more higher-order terms from the series expansions of transcendental functions must be included in the analysis. Zeroth-order approximation^[9] is independent of Λ/λ and can be obtained under the assumption that the displacement vector \mathbf{D} (for $\mathbf{E}\parallel\mathbf{K}$ polarization) and the electric field \mathbf{E} (for $\mathbf{E}\perp\mathbf{K}$ polarization) are approximately constant across the grating period

$$n(m)_{0,E\parallel K} = [(1 - F_m)/n_0^2 + F_m/n_1^2]^{-1/2}, \tag{2}$$

$$n(m)_{0,E\perp K} = [(1 - F_m)n_0^2 + F_m n_1^2]^{1/2}, \tag{3}$$

where F_m is the filling factor of the grating and the subscript '0' indicates the zeroth-order approximation.

In our numerical simulation, however, more precise second-order solutions are used^[7,9]

$$n(m)_{E\parallel K} = \left[n(m)_{0,E\parallel K}^2 + \frac{1}{3} \left(\frac{\Lambda}{\lambda} \right)^2 \pi^2 F_m^2 (1 - F_m)^2 \times \left(\frac{1}{n_1^2} - \frac{1}{n_0^2} \right)^2 n(m)_{0,E\parallel K}^6 n(m)_{0,E\perp K}^2 \right]^{1/2}, \tag{4}$$

$$n(m)_{E\perp K} = \left[n(m)_{0,E\perp K}^2 + \frac{1}{3} \left(\frac{\Lambda}{\lambda} \right)^2 \pi^2 F_m^2 (1 - F_m)^2 \times (n_1^2 - n_0^2)^2 \right]^{1/2}. \tag{5}$$

The characteristic matrix of an assembly of N layers

is^[12]

$$\begin{bmatrix} B \\ C \end{bmatrix} = \left\{ \prod_{m=1}^N \begin{bmatrix} \cos \delta_m & (i \sin \delta_m)/\eta_m \\ i\eta_m \sin \delta_m & \cos \delta_m \end{bmatrix} \right\} \begin{bmatrix} 1 \\ \eta_2 \end{bmatrix}, \tag{6}$$

noindent where $\delta_m = \frac{2\pi d n(m) \cos \theta_m}{N\lambda}$, and

$$\eta_m = y n(m)_{E\perp K} \cos \theta_m \quad (\text{for s - polarisation}), \tag{7}$$

$$\eta_m = y n(m)_{E\parallel K} / \cos \theta_m \quad (\text{for p - polarisation}), \tag{8}$$

where y is the optical admittance in free space, $y = (\epsilon_0/\mu_0)^{1/2} = 2.6544 \times 10^{-3}$ S. If θ_0 , the angle of incidence, is given, the values of θ_m can be found from Snell's law, i.e.,

$$n_0 \sin \theta_0 = n(m) \sin \theta_m = n_2 \sin \theta_2, \tag{9}$$

Let Y be C/B , the reflectance of the triangular shaped grating is

$$R = \left(\frac{\eta_0 - Y}{\eta_0 + Y} \right) \left(\frac{\eta_0 - Y}{\eta_0 + Y} \right)^*. \tag{10}$$

With the formulae above, we could study the characteristics of the triangular shaped grating. Because the grating period Λ and grating depth d are parameters assumed to be under the designer's control, the simple dependence of the zeroth-order indices makes their use with the homogeneous layer in the modeling-design process particularly attractive. However, the use of the second-order and higher order indices in the homogeneous layer model is anticipated to yield more accurate predictions of the grating's behavior. Figure 4 shows the equivalent indices as a function of filling factor with the grating period $\Lambda = 0.5 \mu\text{m}$ and $d = 0.3 \mu\text{m}$ for a grating on glass substrate in air illuminated by $1\text{-}\mu\text{m}$ radiation. At this wavelength the refractive index of glass is approximately 1.5, whereas the extinction coefficient is negligible. These values of $n_{E\parallel K}$ and $n_{E\perp K}$ will be used throughout the remainder of this paper.

As a triangular shaped grating, it has two important structure parameters, period Λ and groove depth d . Figure 5 shows the relation between reflectivity and

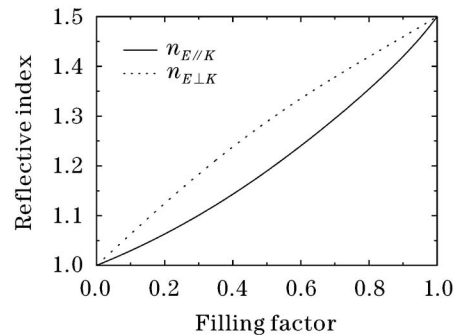


Fig. 4. Equivalent indices of the homogeneous layer model for a grating on glass substrate ($n_1 = 1.5$) in air ($n_0 = 1$). Indices are plotted as a function of filling factor with $\Lambda = 0.5 \mu\text{m}$, $d = 0.3 \mu\text{m}$.

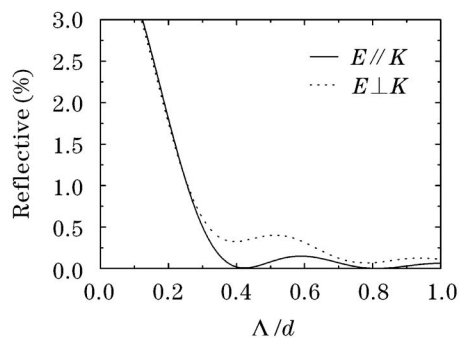


Fig. 5. Relation between reflectivity and groove depth d of the grating. $\lambda = 1 \mu\text{m}$, $\Lambda = 0.5 \mu\text{m}$, $\theta_0 = 0^\circ$.

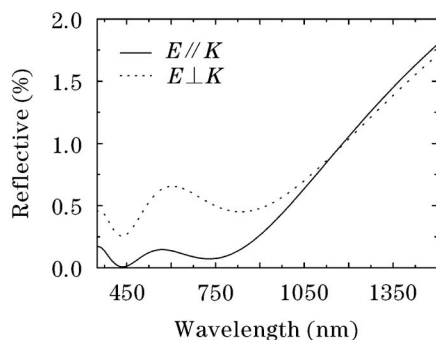


Fig. 6. Diagram of reflectivity in the visible-NIR waveband with parameters: $\Lambda = 0.5 \mu\text{m}$, $d = 0.3 \mu\text{m}$, incident angle $\theta_0 = 0^\circ$.

the groove depth of the grating, with parameters wavelength $\lambda = 1 \mu\text{m}$, $\Lambda = 0.5 \mu\text{m}$, incident angle $\theta_0 = 0^\circ$. To show the results in detail, the y axis was scaled up. We can see that the reflectivity is below 0.5% when Λ/d is between 0.42 and 0.81. Moreover, the reflectivity of the TM wave approximates 0 when Λ/d approximates 0.42 and 0.81. Therefore, we can design the grating with Λ/d between 0.42 and 0.81 to achieve good antireflective properties.

Figure 6 shows the reflectivity curves for this kind of grating in the visible-NIR (near infrared) waveband at normal incidence. We can see that the grating can achieve extremely low reflection for TM wave, which is below 0.3%, to cover the whole visible light waveband. The reflection for a TE wave is higher than that of a TM wave, which is below 0.6% in the visible waveband. This property shows that this kind of grating is very useful to reduce the reflectance of visible light.

The relation of reflectivity versus incident angle θ_0 is shown in Fig. 7. We can see that the triangular shaped grating can achieve extremely low reflectivity for TM and TE waves over the very wide field of incidence. We can get very low reflectance which is less than 0.5% over a broad field of view 60° .

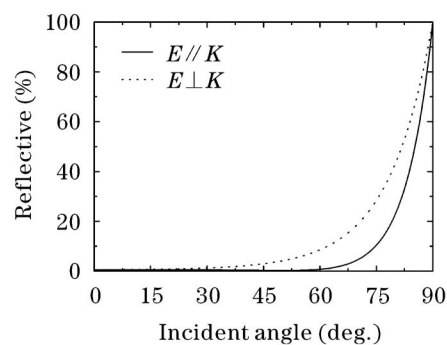


Fig. 7. Reflectivity versus incident angle. $\Lambda = 0.5 \mu\text{m}$, $d = 0.3 \mu\text{m}$, $\lambda = 1 \mu\text{m}$.

In conclusion, the antireflection properties of triangular shaped gratings are studied by a combination of the effective medium theory, and the anisotropic thin-film theory and the results of our computer simulation for the grating are presented. By simulation, we obtained the relations between the reflectivity and the various grating parameters.

We find that this kind of grating can be designed over the whole visible light waveband and it can achieve extremely low reflectance for both TM and TE waves over a broad field of view, which will be very useful when designing a novel optical system.

J. Wang's e-mail address is wjg@siom.ac.cn.

References

1. X. Xu, F. Zhang, and B. Fan, *Acta Opt. Sin.* (in Chinese) **24**, 1173 (2004).
2. T. Yu, F. Zhu, D. Liu, and F. Zhang, *Acta Opt. Sin.* (in Chinese) **25**, 270 (2005).
3. Y. Ono, Y. Kimura, Y. Ohta, and N. Nishida, *Appl. Opt.* **26**, 1142 (1987).
4. M. E. Motamedi, W. H. Southwell, and W. J. Gunning, *Appl. Opt.* **31**, 4371 (1992).
5. T. K. Gaylord, W. E. Baird, and M. G. Moharam, *Appl. Opt.* **25**, 4562 (1986).
6. R. Bräuer and O. Bryngdahl, *Appl. Opt.* **33**, 7875 (1994).
7. D. L. Brundrett, E. N. Glytsis, and T. K. Gaylord, *Appl. Opt.* **33**, 2695 (1994).
8. M. Auslender, D. Levy, and S. Hava, *Appl. Opt.* **37**, 369 (1998).
9. M. Born and E. Wolf, *Principles of Optics* (Cambridge University Press, Cambridge, 1999) p.837.
10. M. A. Golub and A. A. Friesem, *J. Opt. Soc. Am. A* **22**, 1115 (2005).
11. S. M. Rytov, *Sov. Phys. JETP* **2**, 466 (1956).
12. H. A. Macleod, *Thin Film Optical Filters* (Institute of Physics Publishing, Bristol, 2001) p.41.